



1 **Liquid-liquid phase separation in particles containing secondary organic**
2 **material free of inorganic salts**

3

4 Mijung Song^{1,2}, Pengfei Liu³, Scot T. Martin^{3,4}, Allan K. Bertram^{2*}

5 [1] {Department of Earth and Environmental Sciences, Chonbuk National University, Jeollabuk-
6 do, Republic of Korea}

7 [2] {Department of Chemistry, University of British Columbia, Vancouver, BC, V6T 1Z1, Canada}

8 [3] {John A. Paulson School of Engineering and Applied Sciences, Harvard University,
9 Cambridge, Massachusetts 02138, USA}

10 [4] {Department of Earth and Planetary Sciences, Harvard University, Cambridge, Massachusetts
11 02138, USA}

12 Correspondence to: A. K. Bertram (bertram@chem.ubc.ca)

13

14 **Abstract**

15 Particles containing secondary organic material (SOM) are ubiquitous in the atmosphere and play
16 a role in climate and air quality. Recently, research has shown that liquid-liquid phase separation
17 (LLPS) occurs at high relative humidities (RH) (greater than ~ 95 %) in α -pinene-derived SOM
18 particles free of inorganic salts while LLPS does not occur in isoprene-derived SOM particles free
19 of inorganic salts. We expand on these findings by investigating LLPS in SOM particles free of
20 inorganic salts produced from ozonolysis of β -caryophyllene, ozonolysis of limonene, and photo-
21 oxidation of toluene. LLPS was observed at greater than ~95 % RH in the biogenic SOM particles
22 derived from β -caryophyllene and limonene while LLPS was not observed in the anthropogenic
23 SOM particles derived from toluene at 290 ± 1 K. This work combined with the earlier work on
24 LLPS in SOM particles free of inorganic salts suggests that the occurrence of LLPS in SOM
25 particles free of inorganic salts is related to the average oxygen-to-carbon elemental ratio (O:C) of
26 the organic material. When the average O:C is between 0.25 and 0.60, LLPS was observed, but
27 when the average O:C was between 0.52 and 1.3, LLPS was not observed. These results help



1 explain the difference between the hygroscopic parameter κ of SOM particles measured above and
2 below water saturation in the laboratory and field, and have implications for predicting the cloud
3 condensation nucleation properties of SOM particles.

4

5 **1 Introduction**

6 Secondary organic material (SOM) is produced in the atmosphere by the oxidation of volatile
7 organic compounds (VOCs) such as α -pinene and isoprene from trees and toluene from
8 anthropogenic sources. Once formed, the low volatility oxidation products can partition to the
9 particle phase to form SOM containing particles (Hallquist et al., 2009; Ervens et al., 2011). SOM
10 accounts for approximately 20 – 80 % of the submicrometer particle mass in the atmosphere
11 (Zhang et al., 2007; Jimenez et al., 2009). Although the exact chemical composition of SOM in
12 atmospheric particles remains an active area of research, laboratory and field studies have shown
13 that the average oxygen-to-carbon elemental ratio (O:C) of these particles ranges from 0.2 to 1.0
14 (Chen et al., 2009; Jimenez et al., 2009; Heald et al., 2010; Takahama et al., 2011).

15 As the relative humidity (RH) varies in the atmosphere, SOM containing particles can undergo
16 several different phase transitions with implications for the cloud condensation nuclei (CCN)
17 properties, optical properties, reactivity, and growth of these particles (Martin et al., 2000;
18 Raymond and Pandis, 2002; Bilde and Svenningsson, 2004; Zuend et al., 2010; Kuwata and Martin,
19 2012; Brunamonti et al., 2015). One possible phase transition that SOM particles may undergo as
20 RH varies in the atmosphere is liquid-liquid phase separation (LLPS) (Pankow, 2003; Marcolli et
21 al., 2006; Ciobanu et al., 2009; Zuend and Seinfeld, 2012; Veghte et al., 2013; O'Brien et al.,
22 2015). LLPS in particles containing both SOM and inorganic salts has been the focus of many
23 recent studies, and it is now established that SOM particles mixed with inorganic salts can undergo
24 LLPS in the atmosphere when the O:C of the organic material is roughly less than 0.8 (Bertram et
25 al., 2011; Krieger et al., 2012; Smith et al., 2012; Song et al., 2012a; Schill and Tolbert, 2013;
26 Song et al., 2013; You et al., 2013; You et al., 2014).

27 Recently, researchers have also focused on LLPS in SOM particles free of inorganic salts. Peters
28 et al. (2006) suggested that a miscibility gap in particles containing organic polymers at high RH
29 may lead to a non-classical pathway for CCN activation. Renbaum-Wolff et al. (2016) showed that
30 α -pinene-derived SOM free of inorganic salts can undergo LLPS at high RH values (~95 to 100 %)



1 resulting in altered CCN properties. In addition, they showed that LLPS in SOM particles will lead
2 to a different hygroscopic parameter, κ , at subsaturated conditions compared to supersaturated
3 conditions. The implication is that the CCN activity of SOM particles, if they undergo LLPS, is
4 higher than predicted from subsaturated hygroscopicity measurements. Most recently, Rastak et
5 al. (2017) observed that isoprene-derived SOM particles do not undergo LLPS even at high RH.
6 Rastak et al. (2017) also used these results together with thermodynamic calculations to explain
7 the hygroscopic properties of biogenic organic aerosol particles in the laboratory and the field.
8 Here we expand on the studies by Renbaum-Wolff et al. (2016) and Rastak et al. (2017) by
9 investigated LLPS in SOM particles generated by the ozonolysis of limonene, ozonolysis of β -
10 caryophyllene, and photo-oxidation of toluene. Limonene and β -caryophyllene are both biogenic
11 VOCs, while toluene is an anthropogenic VOC (Kanakidou et al., 2005). Both limonene-derived
12 and β -caryophyllene-derived SOM particles have been used as proxies of biogenic SOM particles
13 in the atmosphere (Bateman et al., 2009; Alfarra et al., 2012; Kundu et al., 2012; Frosch et al.,
14 2013; Liu et al., 2013), while toluene-derived SOM has been used as a proxy for anthropogenic
15 SOM particles (Pandis et al., 1992; Robinson et al., 2013; Liu et al., 2016; Song et al., 2016; Ye
16 et al., 2016).

17

18 **2 Methods**

19 **2.1 Production of secondary organic materials**

20 SOM particles were generated via β -caryophyllene ozonolysis and limonene ozonolysis in a flow
21 tube reactor (Table 1) and via toluene photo-oxidation in an oxidation flow reactor (OFR) (Table
22 2). The method of particle generation in the flow tube reactor was described in Shrestha et al.
23 (2013) and the methods of particle generation in the OFR (Kang et al., 2007) were given in Liu et
24 al. (2015). The flow tube reactor was operated at a flow rate of 3.5 L min⁻¹ (with a residence time
25 of 38 s) and < 5% RH. The OFR was operated at flow rates of 7.0 to 9.5 L min⁻¹ (with a residence
26 time of 80 to 110 s) and 13 ± 3 % RH. Both reactors were operated at a temperature of 293 ± 2 K.

27 Table 1 lists the experimental conditions for the production of SOM via ozonolysis. For the particle
28 generation via ozonolysis, ozone was produced by irradiating pure air (Aadco 737 Pure Air
29 Generator) with ultraviolet emission from a mercury lamp ($\lambda = 185$ nm). Ozone concentrations



1 used for ozonolysis ranged from 12 - 30 ppm for β -caryophyllene and 13 - 30 ppm for limonene
2 (Table 1). β -caryophyllene and limonene (Sigma Aldrich, $\geq 99\%$) were dissolved in 2-butanol
3 (Sigma-Aldrich, $\geq 99.5\%$). These organic solutions were injected into a glass round-bottom flask
4 held at 310 K, where the organic liquids vaporized at the tip of a syringe. The organic vapor was
5 then swept into the reactor where ozonolysis took place to form SOM and particles. The injected
6 precursor concentrations were 0.03 - 0.7 ppm for β -caryophyllene and 0.07 - 2.0 ppm for limonene
7 in the main flow of the reactor. In the ozonolysis experiments, butanol served as an OH radical
8 scavenger.

9 Table 2 presents the experimental conditions for the production of SOM via photo-oxidation. For
10 the particle generation via photo-oxidation, hydroxyl radicals were produced in the OFR by the
11 photochemical reactions:



14

15 Ozone was again produced by irradiating pure air (Aadco 737 Pure Air Generator) with ultraviolet
16 emission from a mercury lamp ($\lambda = 185\text{ nm}$). Ozone concentrations used in the photo-oxidation
17 studies were 30 ppm (Table 1). Toluene (Sigma-Aldrich, 99 %) was injected and vaporized in a
18 flask, and the vapors were swept into the OFR by purified air. The injected toluene concentrations
19 were 0.2 - 1.0 ppm.

20

21 **2.2 Production of supermicron SOM particles on hydrophobic substrates**

22 At the outlet of the flow tube reactor and OFR, the sub-micrometer SOM particles were collected
23 on hydrophobic surfaces. The limonene-derived SOM and toluene-derived SOM particles were
24 collected onto glass slides coated with trichloro(1*H*,1*H*,2*H*,2*H*-perfluorooctyl)silane (Sigma-
25 Aldrich, 97%). The coating procedure is described in Knopf (2003). The β -caryophyllene-derived
26 SOM particles were collected onto teflon substrates.



1 Two different methods were used to collect submicron particles on hydrophobic substrates (see
2 Tables 1 and 2). The first method used was an electrostatic precipitator (TSI 3089, USA). In this
3 case, the resulting SOM particles on the hydrophobic substrates were smaller than $\sim 10 \mu\text{m}$. Since
4 particles $20 - 80 \mu\text{m}$ in diameter were required for the LLPS experiments, the following method
5 was used to coagulate the sub- $10 \mu\text{m}$ particles into $20 - 80 \mu\text{m}$ particles: first the substrate
6 containing the SOM particles was placed in a RH-controlled flow-cell (Parsons et al., 2004; Pant
7 et al., 2006; Song et al., 2012b). The RH in the flow-cell was then set to over 100 % for 30 - 60
8 min to grow and coagulate the SOM particles. The RH in the flow-cell was then decreased to ~ 80
9 - 90 % RH to evaporate the water. During the experiments, the particles were observed using a
10 reflectance microscope (Zeiss Axiotech, $50\times$). These growth and coagulation processes resulted in
11 SOM particles consisting of $20 - 80 \mu\text{m}$ in diameter (Song et al., 2015; Renbaum-Wolff et al.,
12 2016).

13 In the second method used to collect SOM particles collected on a hydrophobic substrate, a single
14 stage impactor was used (Prenni et al., 2009; Pöschl et al., 2010; Hosny et al., 2016). In this case,
15 the SOM particles after collection were as big as $100 \mu\text{m}$ due to coagulation during the collection
16 process. Since the particles were already large enough for the LLPS experiments, they were used
17 directly without the need for the growth and coagulation experiments described above. Both
18 methods used to collect SOM particles collected both the water-soluble and water-insoluble
19 components of the SOM particles.

20

21 **2.3 Optical microscopy of supermicron SOM particles**

22 For the LLPS experiments, the hydrophobic substrate containing SOM particles with sizes in the
23 range of 20 to $80 \mu\text{m}$ in diameters was mounted in a temperature and RH controlled flow-cell
24 coupled to an optical reflectance microscope (Zess Axiotech, $50\times$ objective) (Parsons et al., 2004;
25 Pant et al., 2006; Song et al., 2012b). The temperature of the cell was $290 \pm 1 \text{ K}$ in all experiments.
26 RH in the cell was regulated by varying the ratio of a dry and humidified N_2 flow. The total flow
27 rate was $\sim 1200 \text{ sccm}$. The RH was measured using a hygrometer with a chilled mirror sensor
28 (General Eastern, Canada), which was calibrated using the deliquescence RH for pure ammonium
29 sulfate particles (80% RH at 293 K, Martin, 2000). After calibration, the uncertainty of the



1 hygrometer was ± 2.0 % RH. At the beginning of LLPS experiments the SOM particles were
2 equilibrated at ~ 100 % RH for 15 minutes. Then the RH was reduced from ~ 100 to ~ 0 % RH at a
3 rate of 0.1 to 0.5 % RH min^{-1} , and subsequently increased to ~ 100 % RH at a rate of 0.1 to 0.5 %
4 RH min^{-1} . During the humidity cycle, optical images of the SOM particles were recorded every 5
5 - 10 seconds using a CCD camera.

6

7 **3 Results and Discussion**

8 **3.1 β -caryophyllene-derived and limonene-derived SOM particles**

9 Humidity cycles at 290 ± 1 K were performed for β -caryophyllene-derived SOM particles
10 generated with mass concentrations of 15 - 4000 $\mu\text{g m}^{-3}$ and limonene-derived SOM generated
11 with mass concentrations of 80 - 7000 $\mu\text{g m}^{-3}$ (Table 1). In all cases, LLPS was observed at high
12 RH. Table 1 summarizes the results during humidity cycles. Shown in Fig. 1a and Movie S1
13 (Supplementary Material) are examples of optical images of a β -caryophyllene-derived SOM
14 particle as a function of increasing RH for the particle mass concentrations of 2000 - 4000 $\mu\text{g m}^{-3}$.
15 Shown in Fig. 1b and Movie S2 (Supplementary Material) are examples of optical images of a
16 limonene-derived SOM particle as a function of increasing RH for the particle mass concentrations
17 of 7000 $\mu\text{g m}^{-3}$. For both types of SOM particles, only one phase was observed for RH values from
18 0 to ~ 90 %. Note, the light-colored circle in the center of the particles at 90.5 % RH for β -
19 caryophyllene-derived SOM and at 95.0 % RH for limonene-derived SOM is an optical effect due
20 to the light scattering from a hemispherical particle (Bertram et al., 2011). In Fig. 1, LLPS is
21 observed at 91.5 % RH for the β -caryophyllene-derived SOM particle and at 95.3 % RH for the
22 limonene-derived SOM particle. LLPS began with the formation of many small inclusions of a
23 second phase, and in both cases the phase transition occurred over a narrow range of RH. The
24 appearance of many small inclusions is consistent with the phase transition occurring by spinodal
25 decomposition (Ciobanu et al., 2009). Renbaum-Wolff et al. (2016) also observed LLPS in SOM
26 particles produced from α -pinene ozonolysis by spinodal decomposition. The small inclusions
27 coagulated to larger droplets in the β -caryophyllene-derived SOM at 92.5 % RH and in the
28 limonene-derived SOM at 96.1 % RH (Figs. 1a and 1b). The new phase formed is a water-rich
29 phase while the other phase is an SOM-rich phase (Renbaum-Wolff et al., 2016). At the highest
30 RH investigated, the majority of the water-rich phase was in the center of the particles. Such core-



1 shell morphology on a hydrophobic slide glass has been observed previously in dicarboxylic
2 acids/ammonium sulfate/H₂O particles by Song et al. (2012b). After formation of the core-shell
3 morphology consisting of inner and outer phase, the two liquid phases co-existed as high as ~100 %
4 RH. Upon drying, the two liquid phases merge into one liquid phase. This merging process
5 occurred at 90.9 % RH for β -caryophyllene-derived SOM and 95.6 % RH for limonene-derived
6 SOM. Movies of the merging process are shown in the Supplementary Material (Movies S3 and
7 S4).

8 To determine whether the occurrence of LLPS depends on the SOM particle mass concentrations
9 used when generating the SOM, a wide range of the particle mass concentrations covering 15 –
10 7000 $\mu\text{g m}^{-3}$ were investigated (Table 1). Illustrated in Fig. 2a and 2b is the RH at which two
11 phases were observed during humidity cycles as a function of the mass concentrations of the β -
12 caryophyllene-derived and limonene-derived SOM samples. Triangles represent merging relative
13 humidities (MRH) of two liquid phases upon drying and circles represents separation relative
14 humidity (SRH) upon moistening.

15 LLPS was observed at 93.6 ± 1.5 % RH in the β -caryophyllene-derived SOM particles for the
16 particle mass concentrations of 15 – 4000 $\mu\text{g m}^{-3}$ (Fig. 2a). In the limonene-derived SOM particles,
17 LLPS occurred at 96.1 ± 2.1 % RH for the particle mass concentrations of 80 – 7000 $\mu\text{g m}^{-3}$ (Fig.
18 2b). LLPS occurred at 96.0 ± 0.7 % RH in α -pinene-derived SOM particles for the mass
19 concentrations of 75 - 11000 $\mu\text{g m}^{-3}$ (Renbaum-Wolff et al., 2016) (Fig. 2c). As shown in Fig. 2,
20 the SRH and MRH of the β -caryophyllene-derived SOM, limonene-derived SOM, and α -pinene-
21 derived SOM particles do not depend strongly on the SOM particle mass concentrations used to
22 generate the SOM.

23

24 **3.2 Toluene-derived SOM**

25 Humidity cycles were also performed for SOM particles generated from photo-oxidation of
26 toluene, using particle mass concentrations of 80 - 1000 $\mu\text{g m}^{-3}$ in the reactor (Table 2). None of
27 the toluene-derived SOM particles underwent LLPS during RH cycling even at high RH (Table 2).

28 Shown in Fig. 3 and Movie S5 (Supplementary Material) are optical images of toluene-derived
29 SOM particle for the particle mass concentrations of 80 - 100 $\mu\text{g m}^{-3}$. Images in Fig. 3 and Movie



1 S5 were recorded as the RH was increased. No LLPS was observed in the SOM particles during
2 RH cycling between 0 and 100 %. Rastak et al. (2017) did not observed LLPS in isoprene-derived
3 SOM particles for the mass concentrations of 60 - 1000 $\mu\text{g m}^{-3}$

4

5 **3.3 Relation between LLPS and O:C.**

6 Summarized in Table 3 are the average SRH values determined in our work and by Renbaum-
7 Wolff et al. (2016) and Rastak et al. (2017). The average SRH values were based on the SRH
8 values during humidity cycles determined for the different SOM mass concentrations used to
9 generate the SOM since no strong dependence on mass concentrations was apparent. Also included
10 in Table 3 is the range of O:C values previously reported in the literature for the studied SOM
11 particles. Based on the data shown in Table 3, there appears to be a relationship between the
12 occurrence of LLPS and the average O:C of the organic material: when the average O:C was
13 between 0.25 and 0.60, LLPS was observed, but when the average O:C was between 0.52 and 1.3,
14 LLPS was not observed. This trend is also apparent in Fig. 4a, where the data in Table 3 is plotted.

15 The relationship between average O:C and LLPS is consistent with previous studies that explored
16 the miscibility gap in bulk solutions (see Table 1 in Ganbavale et al., 2015). When the average
17 O:C of the organic material was low in a system containing two organic components with water,
18 LLPS was observed. For example, LLPS was observed in a mixture of 1-butanol (O:C = 0.25), 1-
19 propanol (O:C = 0.20), and water (Gomis-Yagües et al., 1998) and in a mixture of 1-pentanol (O:C
20 = 0.20), acetone (O:C=0.33), and water (Tiryaki et al., 1994). On the other hand, when the average
21 O:C of the organic material was high in a system containing two organics and water, LLPS was
22 not observed. For example, LLPS was not observed in a mixture of acetic acid (O:C=1.00), ethanol
23 (O:C=0.50), and water (Pickering, 1893).

24

25 **4. Implications**

26 As mentioned in the introduction, Petters et al. (2006), Renbaum-Wolff et al. (2016), and Rastak
27 et al. (2017) showed using thermodynamic calculations that SOM particles that undergo LLPS at
28 high RH values have modified CCN properties. Hence, LLPS should be considered when



1 predicting the CCN properties of SOM particles derived from α -pinene ozonolysis, β -
2 caryophyllene ozonolysis, and limonene ozonolysis. A caveat is that the mass concentrations used
3 when generating the SOM particles in our experiments was larger than normally found in the
4 atmosphere (Zhang et al., 2007; Jimenez et al., 2009; Spracklen et al., 2011; Li et al., 2015).
5 Additional studies are needed to confirm LLPS in SOM particles generated using more
6 atmospherically relevant SOM mass concentrations.

7 Discrepancy between the hygroscopic parameter, κ , (Petters and Kreidenweis, 2007) measured
8 below water saturation (κ_{HGF}) and above water saturation (κ_{CCN}) in SOM particles have been
9 reported in several studies (Petters et al., 2006; Prenni et al., 2007; Juranyi et al., 2009; Petters et
10 al., 2009; Good et al., 2010; Irwin et al., 2010; Massoli et al., 2010; Dusek et al., 2011; Irwin et
11 al., 2011; Hersey et al., 2013; Pajunoja et al., 2015; Zhao et al., 2016). Petters et al. (2006),
12 Renbaum-Wolff et al. (2016) and Rastak et al. (2017) suggested that such discrepancies are
13 expected in systems that undergo LLPS at high RH. Summarized in Table 4 and Fig. 4b is literature
14 data on the difference between κ_{HGF} and κ_{CCN} (denoted $\Delta\kappa$) as a function of average O:C of the
15 organic material (Prenni et al., 2007; Massoli et al., 2010; Pajunoja et al., 2015). Figure 4b suggests
16 that $\Delta\kappa$ is related to the average O:C of the organic material. Figure 4a and 4b combined suggests
17 that when the average O:C is small, LLPS occurs and the difference between κ_{HGF} and κ_{CCN} is
18 large. On the other hand, when the average O:C is large, LLPS does not occur and the difference
19 between κ_{HGF} and κ_{CCN} is small. Figure 4 provides additional support for the suggestion that the
20 LLPS is related to the discrepancies between κ_{HGF} and κ_{CCN} .

21

22 **Acknowledgments**

23 This work was supported by the Natural Sciences and Engineering Research Council of Canada.
24 Support from the US National Science Foundation (AGS-1640378) and the US Department of
25 Energy (DE-SC0012792) is also acknowledged. Mijung Song acknowledges support from a
26 National Research Foundation of Korea (NRF) grant funded by the Korea Government (MSIP)
27 (2016R1C1B1009243).

28



1 **References**

- 2 Aiken, A. C., Decarlo, P. F., Kroll, J. H., Worsnop, D. R., Huffman, J. A., Docherty, K. S., Ulbrich,
3 I. M., Mohr, C., Kimmel, J. R., Sueper, D., Sun, Y., Zhang, Q., Trimborn, A., Northway, M.,
4 Ziemann, P. J., Canagaratna, M. R., Onasch, T. B., Alfarra, M. R., Prevot, A. S. H., Dommen,
5 J., Duplissy, J., Metzger, A., Baltensperger, U., and Jimenez, J. L.: O/C and OM/OC ratios of
6 primary, secondary, and ambient organic aerosols with high-resolution time-of-flight aerosol
7 mass spectrometry, *Environ. Sci. Technol.*, 42, 4478-4485, Doi 10.1021/Es703009q, 2008.
- 8 Alfarra, M. R., Hamilton, J. F., Wyche, K. P., Good, N., Ward, M. W., Carr, T., Barley, M. H.,
9 Monks, P. S., Jenkin, M. E., Lewis, A. C., and McFiggans, G. B.: The effect of photochemical
10 ageing and initial precursor concentration on the composition and hygroscopic properties of
11 beta-caryophyllene secondary organic aerosol, *Atmos. Chem. Phys.*, 12, 6417-6436,
12 10.5194/acp-12-6417-2012, 2012.
- 13 Bateman, A. P., Nizkorodov, S. A., Laskin, J., and Laskin, A.: Time-resolved molecular
14 characterization of limonene/ozone aerosol using high-resolution electrospray ionization mass
15 spectrometry, *Phys. Chem. Chem. Phys.*, 11, 7931-7942, 10.1039/b905288g, 2009.
- 16 Bertram, A. K., Martin, S. T., Hanna, S. J., Smith, M. L., Bodsworth, A., Chen, Q., Kuwata, M.,
17 Liu, A., You, Y., and Zorn, S. R.: Predicting the relative humidities of liquid-liquid phase
18 separation, efflorescence, and deliquescence of mixed particles of ammonium sulfate, organic
19 material, and water using the organic-to-sulfate mass ratio of the particle and the oxygen-to-
20 carbon elemental ratio of the organic component, *Atmos. Chem. Phys.*, 11, 10995-11006, Doi
21 10.5194/acp-11-10995-2011, 2011.
- 22 Bilde, M., and Svenningsson, B.: CCN activation of slightly soluble organics: the importance of
23 small amounts of inorganic salt and particle phase, *Tellus B*, 56, 128-134, Doi 10.1111/j.1600-
24 0889.2004.00090.x, 2004.
- 25 Brunamonti, S., Krieger, U. K., Marcolli, C., and Peter, T.: Redistribution of black carbon in
26 aerosol particles undergoing liquid-liquid phase separation, *Geophys. Res. Lett.*, 42, 2532-
27 2539, Doi 10.1002/2014gl062908, 2015.



- 1 Chen, Q., Farmer, D. K., Schneider, J., Zorn, S. R., Heald, C. L., Karl, T. G., Guenther, A., Allan,
2 J. D., Robinson, N., Coe, H., Kimmel, J. R., Pauliquevis, T., Borrmann, S., Poschl, U.,
3 Andreae, M. O., Artaxo, P., Jimenez, J. L., and Martin, S. T.: Mass spectral characterization
4 of submicron biogenic organic particles in the Amazon Basin, *Geophys. Res. Lett.*, 36, Artn
5 L2080610.1029/2009gl039880, 2009.
- 6 Chen, Q., Liu, Y. J., Donahue, N. M., Shilling, J. E., and Martin, S. T.: Particle-Phase Chemistry
7 of Secondary Organic Material: Modeled Compared to Measured O:C and H:C Elemental
8 Ratios Provide Constraints, *Environ. Sci. Technol.*, 45, 4763-4770, 10.1021/es104398s, 2011.
- 9 Chhabra, P. S., Ng, N. L., Canagaratna, M. R., Corrigan, A. L., Russell, L. M., Worsnop, D. R.,
10 Flagan, R. C., and Seinfeld, J. H.: Elemental composition and oxidation of chamber organic
11 aerosol, *Atmos. Chem. Phys.*, 11, 8827-8845, 10.5194/acp-11-8827-2011, 2011.
- 12 Ciobanu, V. G., Marcolli, C., Krieger, U. K., Weers, U., and Peter, T.: Liquid-Liquid Phase
13 Separation in Mixed Organic/Inorganic Aerosol Particles, *J. Phys. Chem. A.*, 113, 10966-
14 10978, Doi 10.1021/Jp905054d, 2009.
- 15 Dusek, U., Frank, G. P., Massling, A., Zeromskiene, K., Inuma, Y., Schmid, O., Helas, G., Hennig,
16 T., Wiedensohler, A., and Andreae, M. O.: Water uptake by biomass burning aerosol at sub-
17 and supersaturated conditions: closure studies and implications for the role of organics, *Atmos.*
18 *Chem. Phys.*, 11, 9519-9532, 10.5194/acp-11-9519-2011, 2011.
- 19 Ervens, B., Turpin, B. J., and Weber, R. J.: Secondary organic aerosol formation in cloud droplets
20 and aqueous particles (aqSOA): a review of laboratory, field and model studies, *Atmos. Chem.*
21 *Phys.*, 11, 11069-11102, DOI 10.5194/acp-11-11069-2011, 2011.
- 22 Frosch, M., Bilde, M., Nenes, A., Praplan, A. P., Juranyi, Z., Dommen, J., Gysel, M., Weingartner,
23 E., and Baltensperger, U.: CCN activity and volatility of beta-caryophyllene secondary
24 organic aerosol, *Atmos. Chem. Phys.*, 13, 2283-2297, 10.5194/acp-13-2283-2013, 2013.
- 25 Ganbavale, G., Zuend, A., Marcolli, C., and Peter, T.: Improved AIOMFAC model
26 parameterisation of the temperature dependence of activity coefficients for aqueous organic
27 mixtures, *Atmos. Chem. Phys.*, 15, 447-493, 10.5194/acp-15-447-2015, 2015.



- 1 Gomis-Yagues, V., Ruiz-Bevia, F., Ramos-Nofuentes, M., and Fernandez-Torres, M. J.: The
2 influence of the temperature on the liquid-liquid equilibrium of the ternary system 1-butanol-
3 1-propanol-water, *Fluid Phase Equilib.*, 149, 139-145, Doi 10.1016/S0378-3812(98)00315-
4 X, 1998.
- 5 Good, N., Topping, D. O., Duplissy, J., Gysel, M., Meyer, N. K., Metzger, A., Turner, S. F.,
6 Baltensperger, U., Ristovski, Z., Weingartner, E., Coe, H., and McFiggans, G.: Widening the
7 gap between measurement and modelling of secondary organic aerosol properties?, *Atmos.*
8 *Chem. Phys.*, 10, 2577-2593, 10.5194/acp-10-2577-2010, 2010.
- 9 Hallquist, M., Wenger, J. C., Baltensperger, U., Rudich, Y., Simpson, D., Claeys, M., Dommen,
10 J., Donahue, N. M., George, C., Goldstein, A. H., Hamilton, J. F., Herrmann, H., Hoffmann,
11 T., Iinuma, Y., Jang, M., Jenkin, M. E., Jimenez, J. L., Kiendler-Scharr, A., Maenhaut, W.,
12 McFiggans, G., Mentel, T. F., Monod, A., Prevot, A. S. H., Seinfeld, J. H., Surratt, J. D.,
13 Szmigielski, R., and Wildt, J.: The formation, properties and impact of secondary organic
14 aerosol: current and emerging issues, *Atmos. Chem. Phys.*, 9, 5155-5236, 2009.
- 15 Heald, C. L., Kroll, J. H., Jimenez, J. L., Docherty, K. S., DeCarlo, P. F., Aiken, A. C., Chen, Q.,
16 Martin, S. T., Farmer, D. K., and Artaxo, P.: A simplified description of the evolution of
17 organic aerosol composition in the atmosphere, *Geophys. Res. Lett.*, 37, -, Artn L08803, Doi
18 10.1029/2010gl042737, 2010.
- 19 Heaton, K. J., Dreyfus, M. A., Wang, S., and Johnston, M. V.: Oligomers in the early stage of
20 biogenic secondary organic aerosol formation and growth, *Environ. Sci. Technol.*, 41, 6129-
21 6136, 10.1021/es070314n, 2007.
- 22 Hersey, S. P., Craven, J. S., Metcalf, A. R., Lin, J., Lathem, T., Suski, K. J., Cahill, J. F., Duong,
23 H. T., Sorooshian, A., Jonsson, H. H., Shiraiwa, M., Zuend, A., Nenes, A., Prather, K. A.,
24 Flagan, R. C., and Seinfeld, J. H.: Composition and hygroscopicity of the Los Angeles Aerosol:
25 CalNex, *J. Geophys. Res.-Atmos.*, 118, 3016-3036, 10.1002/jgrd.50307, 2013.
- 26 Hosny, N. A., Fitzgerald, C., Vysniauskas, A., Athanasiadis, A., Berkemeier, T., Uygur, N., Poschl,
27 U., Shiraiwa, M., Kalberer, M., Pope, F. D., and Kuimova, M. K.: Direct imaging of changes



- 1 in aerosol particle viscosity upon hydration and chemical aging, *Chem. Sci.*, 7, 1357-1367,
2 10.1039/c5sc02959g, 2016.
- 3 Irwin, M., Good, N., Crosier, J., Choularton, T. W., and McFiggans, G.: Reconciliation of
4 measurements of hygroscopic growth and critical supersaturation of aerosol particles in
5 central Germany, *Atmos. Chem. Phys.*, 10, 11737-11752, 10.5194/acp-10-11737-2010, 2010.
- 6 Irwin, M., Robinson, N., Allan, J. D., Coe, H., and McFiggans, G.: Size-resolved aerosol water
7 uptake and cloud condensation nuclei measurements as measured above a Southeast Asian
8 rainforest during OP3, *Atmos. Chem. Phys.*, 11, 11157-11174, 10.5194/acp-11-11157-2011,
9 2011.
- 10 Jimenez, J. L., Canagaratna, M. R., Donahue, N. M., Prevot, A. S. H., Zhang, Q., Kroll, J. H.,
11 DeCarlo, P. F., Allan, J. D., Coe, H., Ng, N. L., Aiken, A. C., Docherty, K. S., Ulbrich, I. M.,
12 Grieshop, A. P., Robinson, A. L., Duplissy, J., Smith, J. D., Wilson, K. R., Lanz, V. A.,
13 Hueglin, C., Sun, Y. L., Tian, J., Laaksonen, A., Raatikainen, T., Rautiainen, J., Vaattovaara,
14 P., Ehn, M., Kulmala, M., Tomlinson, J. M., Collins, D. R., Cubison, M. J., Dunlea, E. J.,
15 Huffman, J. A., Onasch, T. B., Alfarra, M. R., Williams, P. I., Bower, K., Kondo, Y.,
16 Schneider, J., Drewnick, F., Borrmann, S., Weimer, S., Demerjian, K., Salcedo, D., Cottrell,
17 L., Griffin, R., Takami, A., Miyoshi, T., Hatakeyama, S., Shimono, A., Sun, J. Y., Zhang, Y.
18 M., Dzepina, K., Kimmel, J. R., Sueper, D., Jayne, J. T., Herndon, S. C., Trimborn, A. M.,
19 Williams, L. R., Wood, E. C., Middlebrook, A. M., Kolb, C. E., Baltensperger, U., and
20 Worsnop, D. R.: Evolution of Organic Aerosols in the Atmosphere, *Science*, 326, 1525-1529,
21 Doi 10.1126/science.1180353, 2009.
- 22 Juranyi, Z., Gysel, M., Duplissy, J., Weingartner, E., Tritscher, T., Dommen, J., Henning, S., Ziese,
23 M., Kiselev, A., Stratmann, F., George, I., and Baltensperger, U.: Influence of gas-to-particle
24 partitioning on the hygroscopic and droplet activation behaviour of alpha-pinene secondary
25 organic aerosol, *Phys. Chem. Chem. Phys.*, 11, 8091-8097, Doi 10.1039/B904162a, 2009.
- 26 Kanakidou, M., Seinfeld, J. H., Pandis, S. N., Barnes, I., Dentener, F. J., Facchini, M. C., Van
27 Dingenen, R., Ervens, B., Nenes, A., Nielsen, C. J., Swietlicki, E., Putaud, J. P., Balkanski,
28 Y., Fuzzi, S., Horth, J., Moortgat, G. K., Winterhalter, R., Myhre, C. E. L., Tsigaridis, K.,



- 1 Vignati, E., Stephanou, E. G., and Wilson, J.: Organic aerosol and global climate modelling:
2 a review, *Atmos. Chem. Phys.*, 5, 1053-1123, 2005.
- 3 Kang, E., Root, M. J., Toohey, D. W., and Brune, W. H.: Introducing the concept of Potential
4 Aerosol Mass (PAM), *Atmos. Chem. Phys.*, 7, 5727-5744, 2007.
- 5 Knopf, D. A.: Thermodynamic properties and nucleation processes of upper tropospheric and
6 lower stratospheric aerosol particles, Diss. ETH No. 15103, Zurich, Switzerland, 2003.
- 7 Krieger, U. K., Marcolli, C., and Reid, J. P.: Exploring the complexity of aerosol particle properties
8 and processes using single particle techniques, *Chem. Soc. Rev.*, 41, 6631-6662,
9 10.1039/c2cs35082c, 2012.
- 10 Kundu, S., Fisseha, R., Putman, A. L., Rahn, T. A., and Mazzoleni, L. R.: High molecular weight
11 SOA formation during limonene ozonolysis: insights from ultrahigh-resolution FT-ICR mass
12 spectrometry characterization, *Atmos. Chem. Phys.*, 12, 5523-5536, 10.5194/acp-12-5523-
13 2012, 2012.
- 14 Kuwata, M., and Martin, S. T.: Phase of atmospheric secondary organic material affects its
15 reactivity, *P. Natl. Acad. Sci. USA*, 109, 17354-17359, 10.1073/pnas.1209071109, 2012.
- 16 Lambe, A. T., Chhabra, P. S., Onasch, T. B., Brune, W. H., Hunter, J. F., Kroll, J. H., Cummings,
17 M. J., Brogan, J. F., Parmar, Y., Worsnop, D. R., Kolb, C. E., and Davidovits, P.: Effect of
18 oxidant concentration, exposure time, and seed particles on secondary organic aerosol
19 chemical composition and yield, *Atmos. Chem. Phys.*, 15, 3063-3075, 10.5194/acp-15-3063-
20 2015, 2015.
- 21 Li, Y. J., Lee, B. P., Su, L., Fung, J. C. H., and Chan, C. K.: Seasonal characteristics of fine
22 particulate matter (PM) based on high-resolution time-of-flight aerosol mass spectrometric
23 (HR-ToF-AMS) measurements at the HKUST Supersite in Hong Kong, *Atmos. Chem. Phys.*,
24 15, 37-53, 10.5194/acp-15-37-2015, 2015.
- 25 Liu, P. F., Abdelmalki, N., Hung, H. M., Wang, Y., Brune, W. H., and Martin, S. T.: Ultraviolet
26 and visible complex refractive indices of secondary organic material produced by
27 photooxidation of the aromatic compounds toluene and m-xylene, *Atmos. Chem. Phys.*, 15,
28 1435-1446, 10.5194/acp-15-1435-2015, 2015.



- 1 Liu, P. F., Li, Y. J., Wang, Y., Gilles, M. K., Zaveri, R. A., Bertram, A. K., and Martin, S. T.:
2 Labiality of secondary organic particulate matter, *P. Natl. Acad. Sci. USA*, 113, 12643-12648,
3 10.1073/pnas.1603138113, 2016.
- 4 Liu, P. F., Zhang, Y., and Martin, S. T.: Complex Refractive Indices of Thin Films of Secondary
5 Organic Materials by Spectroscopic Ellipsometry from 220 to 1200 nm, *Environ. Sci.*
6 *Technol.*, 47, 13594-13601, Doi 10.1021/Es403411e, 2013.
- 7 Marcolli, C., and Krieger, U. K.: Phase changes during hygroscopic cycles of mixed
8 organic/inorganic model systems of tropospheric aerosols, *J. Phys. Chem. A.*, 110, 1881-1893,
9 Doi 10.1021/Jp0556759, 2006.
- 10 Martin, S. T.: Phase transitions of aqueous atmospheric particles, *Chem. Rev.*, 100, 3403-3453,
11 Doi 10.1021/Cr990034t, 2000.
- 12 Massoli, P., Lambe, A. T., Ahern, A. T., Williams, L. R., Ehn, M., Mikkila, J., Canagaratna, M.
13 R., Brune, W. H., Onasch, T. B., Jayne, J. T., Petaja, T., Kulmala, M., Laaksonen, A., Kolb,
14 C. E., Davidovits, P., and Worsnop, D. R.: Relationship between aerosol oxidation level and
15 hygroscopic properties of laboratory generated secondary organic aerosol (SOA) particles,
16 *Geophys. Res. Lett.*, 37, Artn L2480110.1029/2010gl045258, 2010.
- 17 O'Brien, R. E., Wang, B. B., Kelly, S. T., Lundt, N., You, Y., Bertram, A. K., Leone, S. R., Laskin,
18 A., and Gilles, M. K.: Liquid-liquid phase separation in aerosol particles: Imaging at the
19 nanometer scale, *Environ. Sci. Technol.*, 49, 4995-5002, 10.1021/acs.est.5b00062, 2015.
- 20 Pajunoja, A., Lambe, A. T., Hakala, J., Rastak, N., Cummings, M. J., Brogan, J. F., Hao, L. Q.,
21 Paramonov, M., Hong, J., Prisle, N. L., Malila, J., Romakkaniemi, S., Lehtinen, K. E. J.,
22 Laaksonen, A., Kulmala, M., Massoli, P., Onasch, T. B., Donahue, N. M., Riipinen, I.,
23 Davidovits, P., Worsnop, D. R., Petaja, T., and Virtanen, A.: Adsorptive uptake of water by
24 semisolid secondary organic aerosols, *Geophys. Res. Lett.*, 42, 3063-3068, Doi
25 10.1002/2015gl063142, 2015.
- 26 Pandis, S. N., Harley, R. A., Cass, G. R., and Seinfeld, J. H.: Secondary organic aerosol formation
27 and transport, *Atmos. Environ. a-Gen*, 26, 2269-2282, Doi 10.1016/0960-1686(92)90358-R,
28 1992.



- 1 Pankow, J. F.: Gas/particle partitioning of neutral and ionizing compounds to single and multi-
2 phase aerosol particles. 1. Unified modeling framework, *Atmos. Environ.*, 37, 3323-3333, Doi
3 10.1016/S1352-2310(03)00346-7, 2003.
- 4 Pant, A., Parsons, M. T., and Bertram, A. K.: Crystallization of aqueous ammonium sulfate
5 particles internally mixed with soot and kaolinite: Crystallization relative humidities and
6 nucleation rates, *J. Phys. Chem. A.*, 110, 8701-8709, Doi 10.1021/Jp060985s, 2006.
- 7 Parsons, M. T., Mak, J., Lipetz, S. R., and Bertram, A. K.: Deliquescence of malonic, succinic,
8 glutaric, and adipic acid particles, *J. Geophys. Res.-Atmos.*, 109, -, Artn D06212, Doi
9 10.1029/2003jd004075, 2004.
- 10 Petters, M. D., Kreidenweis, S. M., Snider, J. R., Koehler, K. A., Wang, Q., Prenni, A. J., and
11 Demott, P. J.: Cloud droplet activation of polymerized organic aerosol, *Tellus B*, 58, 196-205,
12 DOI 10.1111/j.1600-0889.2006.00181.x, 2006.
- 13 Petters, M. D., and Kreidenweis, S. M.: A single parameter representation of hygroscopic growth
14 and cloud condensation nucleus activity, *Atmos. Chem. Phys.*, 7, 1961-1971, 2007.
- 15 Petters, M. D., Wex, H., Carrico, C. M., Hallbauer, E., Massling, A., McMeeking, G. R., Poulain,
16 L., Wu, Z., Kreidenweis, S. M., and Stratmann, F.: Towards closing the gap between
17 hygroscopic growth and activation for secondary organic aerosol - Part 2: Theoretical
18 approaches, *Atmos. Chem. Phys.*, 9, 3999-4009, 2009.
- 19 Pickering, S.: LXXI. A study of the properties of some strong solutions, *J. Chem. Soc.*, 63, 998-
20 1027, 1893.
- 21 Pöschl, U., Martin, S. T., Sinha, B., Chen, Q., Gunthe, S. S., Huffman, J. A., Borrmann, S., Farmer,
22 D. K., Garland, R. M., Helas, G., Jimenez, J. L., King, S. M., Manzi, A., Mikhailov, E.,
23 Pauliquevis, T., Petters, M. D., Prenni, A. J., Roldin, P., Rose, D., Schneider, J., Su, H., Zorn,
24 S. R., Artaxo, P., and Andreae, M. O.: Rainforest aerosols as biogenic nuclei of clouds and
25 precipitation in the Amazon, *Science*, 329, 1513-1516, Doi 10.1126/science.1191056, 2010.
- 26 Prenni, A. J., Petters, M. D., Kreidenweis, S. M., DeMott, P. J., and Ziemann, P. J.: Cloud droplet
27 activation of secondary organic aerosol, *J. Geophys. Res.-Atmos.*, 112, Artn D10223, Doi
28 10.1029/2006jd007963, 2007.



- 1 Prenni, A. J., Petters, M. D., Kreidenweis, S. M., Heald, C. L., Martin, S. T., Artaxo, P., Garland,
2 R. M., Wollny, A. G., and Poschl, U.: Relative roles of biogenic emissions and Saharan dust
3 as ice nuclei in the Amazon basin, *Nat. Geosci.*, 2, 401-404, Doi 10.1038/Ngeo517, 2009.
- 4 Rastak, N., A. Pajunoja, J. C. Acosta Navarro, D. G. Partridge, J. Ma, M. Song, A. Kirkevåg, Y.
5 Leong, W. W. Hu, N. F. Taylor, D. R. Collins, K. Cerully, A. Bougagioti, R. Krejci, P. Liu,
6 T. Petäjä, C. Percival, A. M. L. Ekman, A. Nenes, S. T. Martin, J. L. Jimenez, D. O. Topping,
7 A. K. Bertram, A. Zuend, A. Virtanen, and I. Riipinen: Microphysical explanation of the RH-
8 dependent water-affinity of biogenic organic aerosol and its importance for climate, *Geophys.*
9 *Res. Lett.*, accepted, 2017.
- 10 Raymond, T. M., and Pandis, S. N.: Cloud activation of single-component organic aerosol particles,
11 *J. Geophys. Res.-Atmos.*, 107, Artn 478710.1029/2002jd002159, 2002.
- 12 Reinhardt, A., Emmenegger, C., Gerrits, B., Panse, C., Dommen, J., Baltensperger, U., Zenobi, R.,
13 and Kalberer, M.: Ultrahigh mass resolution and accurate mass measurements as a tool to
14 characterize oligomers in secondary organic aerosols, *Anal. Chem.*, 79, 4074-4082,
15 10.1021/ac062425v, 2007.
- 16 Renbaum-Wolff, L., Song, M. J., Marcolli, C., Zhang, Y., Liu, P. F. F., Grayson, J. W., Geiger, F.
17 M., Martin, S. T., and Bertram, A. K.: Observations and implications of liquid-liquid phase
18 separation at high relative humidities in secondary organic material produced by alpha-pinene
19 ozonolysis without inorganic salts, *Atmos. Chem. Phys.*, 16, 7969-7979, 10.5194/acp-16-
20 7969-2016, 2016.
- 21 Robinson, E. S., Saleh, R., and Donahue, N. M.: Organic aerosol mixing observed by single-
22 particle mass spectrometry, *J. Phys. Chem. A.*, 117, 13935-13945, 10.1021/jp405789t, 2013.
- 23 Schill, G. P., and Tolbert, M. A.: Heterogeneous ice nucleation on phase-separated organic-sulfate
24 particles: effect of liquid vs. glassy coatings, *Atmos. Chem. Phys.*, 13, 4681-4695,
25 10.5194/acp-13-4681-2013, 2013.
- 26 Shrestha, M., Zhang, Y., Ebben, C. J., Martin, S. T., and Geiger, F. M.: Vibrational sum frequency
27 generation spectroscopy of secondary organic material produced by condensational growth



- 1 from alpha-pinene ozonolysis, *J. Phys. Chem. A.*, 117, 8427-8436, Doi 10.1021/Jp405065d,
2 2013.
- 3 Smith, M. L., Bertram, A. K., and Martin, S. T.: Deliquescence, efflorescence, and phase
4 miscibility of mixed particles of ammonium sulfate and isoprene-derived secondary organic
5 material, *Atmos. Chem. Phys.*, 12, 9613-9628, 10.5194/acp-12-9613-2012, 2012.
- 6 Song, M., Marcolli, C., Krieger, U. K., Zuend, A., and Peter, T.: Liquid-liquid phase separation
7 and morphology of internally mixed dicarboxylic acids/ammonium sulfate/water particles,
8 *Atmos. Chem. Phys.*, 12, 2691-2712, Doi 10.5194/acp-12-2691-2012, 2012b.
- 9 Song, M., Marcolli, C., Krieger, U. K., Zuend, A., and Peter, T.: Liquid-liquid phase separation in
10 aerosol particles: Dependence on O:C, organic functionalities, and compositional complexity,
11 *Geophys. Res. Lett.*, 39, Artn L19801, Doi 10.1029/2012gl052807, 2012a.
- 12 Song, M. J., Marcolli, C., Krieger, U. K., Lienhard, D. M., and Peter, T.: Morphologies of mixed
13 organic/inorganic/aqueous aerosol droplets, *Faraday Discuss.*, 165, 289-316, Doi
14 10.1039/C3fd00049d, 2013.
- 15 Song, M., Liu, P. F., Hanna, S. J., Li, Y. J., Martin, S. T., and Bertram, A. K.: Relative humidity-
16 dependent viscosities of isoprene-derived secondary organic material and atmospheric
17 implications for isoprene-dominant forests, *Atmos. Chem. Phys.*, 15, 5145-5159, Doi
18 10.5194/acp-15-5145-2015, 2015.
- 19 Spracklen, D. V., Jimenez, J. L., Carslaw, K. S., Worsnop, D. R., Evans, M. J., Mann, G. W.,
20 Zhang, Q., Canagaratna, M. R., Allan, J., Coe, H., McFiggans, G., Rap, A., and Forster, P.:
21 Aerosol mass spectrometer constraint on the global secondary organic aerosol budget, *Atmos.*
22 *Chem. Phys.*, 11, 12109-12136, 10.5194/acp-11-12109-2011, 2011.
- 23 Takahama, S., Schwartz, R. E., Russell, L. M., Macdonald, A. M., Sharma, S., and Leaitch, W. R.:
24 Organic functional groups in aerosol particles from burning and non-burning forest emissions
25 at a high-elevation mountain site, *Atmos. Chem. Phys.*, 11, 6367-6386, Doi 10.5194/acp-11-
26 6367-2011, 2011.



- 1 Tiryaki, A., Guruz, G., and Orbey, H.: Liquid-Liquid Equilibria of Ternary-Systems of Water Plus
2 Acetone and C-5-Alcohol and C-8-Alcohol at 298-K, 303-K and 308-K, Fluid Phase Equilibr.,
3 94, 267-280, Doi 10.1016/0378-3812(94)87061-6, 1994.
- 4 Veghte, D. P., Altaf, M. B., and Freedman, M. A.: Size Dependence of the Structure of Organic
5 Aerosol, J. Am. Chem. Soc., 135, 16046-16049, 10.1021/ja408903g, 2013.
- 6 Ye, Q., Robinson, E. S., Ding, X., Ye, P. L., Sullivan, R. C., and Donahue, N. M.: Mixing of
7 secondary organic aerosols versus relative humidity, P. Natl. Acad. Sci. USA, 113, 12649-
8 12654, 10.1073/pnas.1604536113, 2016.
- 9 You, Y., Renbaum-Wolff, L., and Bertram, A. K.: Liquid-liquid phase separation in particles
10 containing organics mixed with ammonium sulfate, ammonium bisulfate, ammonium nitrate
11 or sodium chloride, Atmos. Chem. Phys., 13, 11723-11734, 10.5194/acp-13-11723-2013,
12 2013.
- 13 You, Y., Smith, M. L., Song, M. J., Martin, S. T., and Bertram, A. K.: Liquid-liquid phase
14 separation in atmospherically relevant particles consisting of organic species and inorganic
15 salts, Int. Rev. Phys. Chem., 33, 43-77, 10.1080/0144235X.2014.890786, 2014.
- 16 Zhang, Q., Jimenez, J. L., Canagaratna, M. R., Allan, J. D., Coe, H., Ulbrich, I., Alfarra, M. R.,
17 Takami, A., Middlebrook, A. M., Sun, Y. L., Dzepina, K., Dunlea, E., Docherty, K., DeCarlo,
18 P. F., Salcedo, D., Onasch, T., Jayne, J. T., Miyoshi, T., Shimonono, A., Hatakeyama, S.,
19 Takegawa, N., Kondo, Y., Schneider, J., Drewnick, F., Borrmann, S., Weimer, S., Demerjian,
20 K., Williams, P., Bower, K., Bahreini, R., Cottrell, L., Griffin, R. J., Rautiainen, J., Sun, J. Y.,
21 Zhang, Y. M., and Worsnop, D. R.: Ubiquity and dominance of oxygenated species in organic
22 aerosols in anthropogenically-influenced Northern Hemisphere midlatitudes, Geophys. Res.
23 Lett., 34, Artn L13801, Doi 10.1029/2007gl029979, 2007.
- 24 Zhao, D. F., Buchholz, A., Kortner, B., Schlag, P., Rubach, F., Fuchs, H., Kiendler-Scharr, A.,
25 Tillmann, R., Wahner, A., Watne, A. K., Hallquist, M., Flores, J. M., Rudich, Y., Kristensen,
26 K., Hansen, A. M. K., Glasius, M., Kourtev, I., Kalberer, M., and Mentel, T. F.: Cloud
27 condensation nuclei activity, droplet growth kinetics, and hygroscopicity of biogenic and



1 anthropogenic secondary organic aerosol (SOA), Atmos. Chem. Phys., 16, 1105-1121,
2 10.5194/acp-16-1105-2016, 2016.

3 Zuend, A., Marcolli, C., Peter, T., and Seinfeld, J. H.: Computation of liquid-liquid equilibria and
4 phase stabilities: implications for RH-dependent gas/particle partitioning of organic-inorganic
5 aerosols, Atmos. Chem. Phys., 10, 7795-7820, Doi 10.5194/acp-10-7795-2010, 2010.

6 Zuend, A., and Seinfeld, J. H.: Modeling the gas-particle partitioning of secondary organic aerosol:
7 the importance of liquid-liquid phase separation, Atmos. Chem. Phys., 12, 3857-3882,
8 10.5194/acp-12-3857-2012, 2012.

9



- 1 Table 1. Experimental conditions for produced and collection of SOM particles by ozonolysis and
- 2 measured separation relative humidities (SRH) upon moistening and merging relative humidities
- 3 (MRH) upon drying of the collected particles. Particles were collected on hydrophobic substrates
- 4 using an electrostatic precipitator or single stage impactor.

SOM sample	VOC conc. (ppm)	O ₃ conc. (ppm)	SOM mass conc. (μg m ⁻³)	Flow rate for SOM particle production (L m ⁻¹)	Collection time (hour)	Collection method	MRH (%)	SRH (%)
β-caryophyllene 1	0.03	30	15-30	7.0	24	Single stage impactor	92.7	94.9
β-caryophyllene 2	0.03	30	15-30	7.0	46	Single stage impactor	95.0	94.4
β-caryophyllene 3	0.7	12	2000-4000	3.5	6	Electrostatic precipitator	90.9	91.5
β-caryophyllene 4	0.7	12	2000-4000	3.5	14	Electrostatic precipitator	93.9	94.1
β-caryophyllene 5	0.7	12	2000-4000	3.5	9	Electrostatic precipitator	93.9	94.1
Limonene 1	0.07	30	80-90	7.0	24	Single stage impactor	95.6	98.7
Limonene 2	0.07	30	80-90	7.0	24	Single stage impactor	97.4	98.8
Limonene 3	2.0	13	7000	3.5	20	Electrostatic precipitator	95.6	95.3
Limonene 4	2.0	13	7000	3.5	20	Electrostatic precipitator	92.7	94.5

5

6



- 1 Table 2. Experimental conditions for production and collection of SOM produced by photo-
 2 oxidation and measured separation relative humidities (SRH) upon moistening and merging
 3 relative humidities (MRH) upon drying of the collected particles. Particles were collected on
 4 hydrophobic substrates using an electrostatic precipitator or single stage impactor. SRH = 0 and
 5 MRH = 0 indicates LLPS was not observed during humidity cycles.

SOM sample	VOC conc. (ppm)	O ₃ conc. (ppm)	SOM mass conc. (µg m ⁻³)	Flow rate for SOM particle production (L m ⁻¹)	Collection time (hour)	Collection method	MRH (%)	SRH (%)
Toluene 1	0.2	30	80-100	7.0	20	Single stage impactor	0	0
Toluene 2	0.2	30	80-100	7.0	24	Single stage impactor	0	0
Toluene 3	1.0	30	600-1000	7.0	48	Electrostatic precipitator	0	0
Toluene 4	1.0	30	600-1000	7.0	48	Electrostatic precipitator	0	0
Toluene 5	1.0	30	600-1000	7.0	96	Electrostatic precipitator	0	0
Toluene 6	1.0	30	600-1000	7.0	96	Electrostatic precipitator	0	0

6

7



1 Table 3. Summary of the LLPS results as well as the oxygen-to-carbon atomic ratios (O:C) of the
2 studied SOM particles. The standard deviation (σ) of the separation relative humidity (SRH) and
3 merging relative humidities (MRH) is derived from several cycles of RH for different SOM mass
4 concentrations. SRH = 0 and MRH = 0 indicates phase separation was absent in particles.

SOM	O:C range of SOM		Average RH (%) $\pm \sigma$	
	Lowest	Highest	MRH	SRH
Ozonolysis of β -caryophyllene	0.25 ^a	0.45 ^a	93.3 \pm 1.7	93.8 \pm 1.3
Ozonolysis of α -pinene	0.27 ^b	0.60 ^c	95.9 \pm 0.8 ^d	96.1 \pm 0.6 ^d
Ozonolysis of limonene	0.34 ^e	0.47 ^f	95.3 \pm 1.9	96.8 \pm 2.2
Photo-oxidation of isoprene	0.52 ^g	0.85 ^g	0 ^h	0 ^h
Photo-oxidation of toluene	0.68 ⁱ	1.32 ^g	0	0

5 ^aChen et al. (2011); ^bAiken et al. (2008); ^cReinhardt et al. (2007); ^dRenbaum-Wolff et al. (2016);
6 ^eHeaton et al. (2007); ^fBateman et al. (2009); ^gLambe et al. (2015); ^hRastak et al. (2017); ⁱChhabra
7 et al. (2011)

8

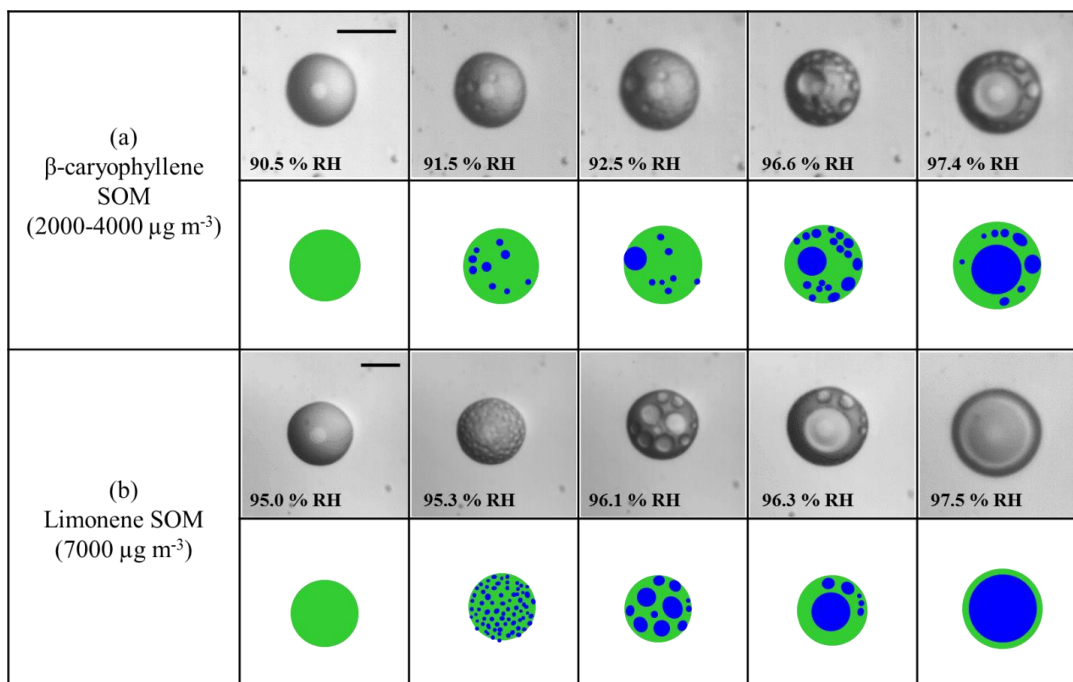


- 1 Table 4. Literature data of measured O:C ratio, κ_{HGF} , κ_{CCN} , and the difference between κ_{HGF} and
 2 κ_{CCN} , denoted as $\Delta\kappa$, of SOMs.

SOM	O:C	κ_{HGF}	κ_{CCN}	$\Delta\kappa$	Reference
	at 90% RH				
Photo-oxidation of α -pinene	0.4	0.04	0.15	0.11	Massoli et al. (2010)
	0.43	0.07	0.16	0.09	Massoli et al. (2010)
	0.45	0.03	0.11	0.08	Pajunoja et al. (2015)
	0.55	0.10	0.12	0.02	Pajunoja et al. (2015)
	0.67	0.14	0.18	0.04	Massoli et al. (2010)
	0.70	0.12	0.13	0.01	Pajunoja et al. (2015)
Photo-oxidation of isoprene	0.86	0.13	0.14	0.01	Pajunoja et al. (2015)
Photo-oxidation of longifolene	0.39	0.02	0.10	0.08	Pajunoja et al. (2015)
	0.56	0.03	0.09	0.06	Pajunoja et al. (2015)
	0.83	0.08	0.10	0.02	Pajunoja et al. (2015)

3

4



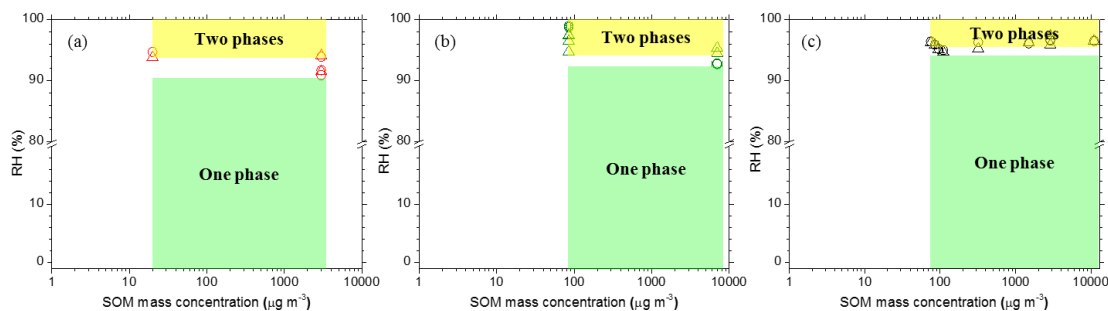
1

2

3 Figure 1. Optical images of SOM particles with increasing RH: (a) β-caryophyllene-derived SOM
 4 for the mass concentrations of 2000 - 4000 μg m⁻³ (β-caryophyllene 3, Table 1) and (b) limonene-
 5 derived SOM for the mass concentrations of 7000 μg m⁻³ (Limonene 3, Table 1). Note that the
 6 light gray circles at the center of the particles are an optical effect due to the hemispherical nature
 7 of the particles. Illustrations are shown below the images for clarity. Green: SOM-rich phase. Blue:
 8 water-rich phase. The scale bar is 20 μm.

9

10

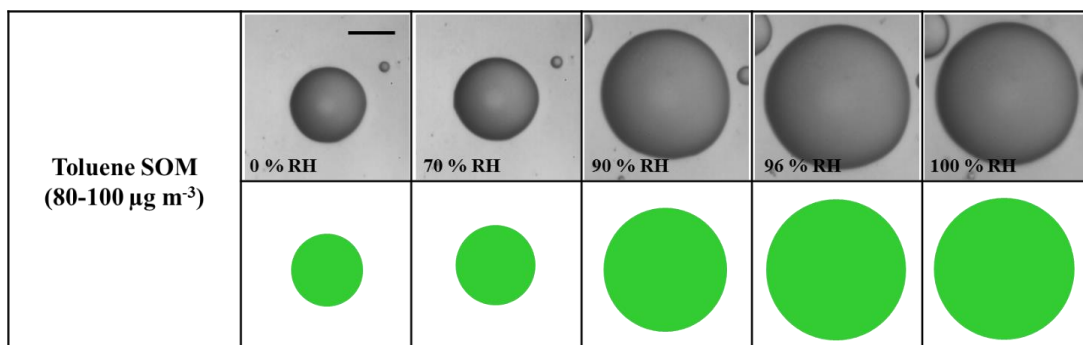


1

2

3 Figure 2. RH at which two phases were observed during humidity cycles of individual particles of
4 (a) β -caryophyllene-derived SOM and (b) limonene-derived SOM from this study, and (c) α -
5 pinene-derived SOM from Renbaum-Wolff et al. (2016) as a function of the SOM mass
6 concentrations. For all panels, circles represent onset of phase separation upon moistening (i.e.
7 separation relative humidity, SRH) and triangles represent merging of two liquid phases upon
8 drying (i.e. merging relative humidity, MRH). Yellow shaded region indicates two phases present
9 and green shaded region indicates one phase prevalent in SOM.

10



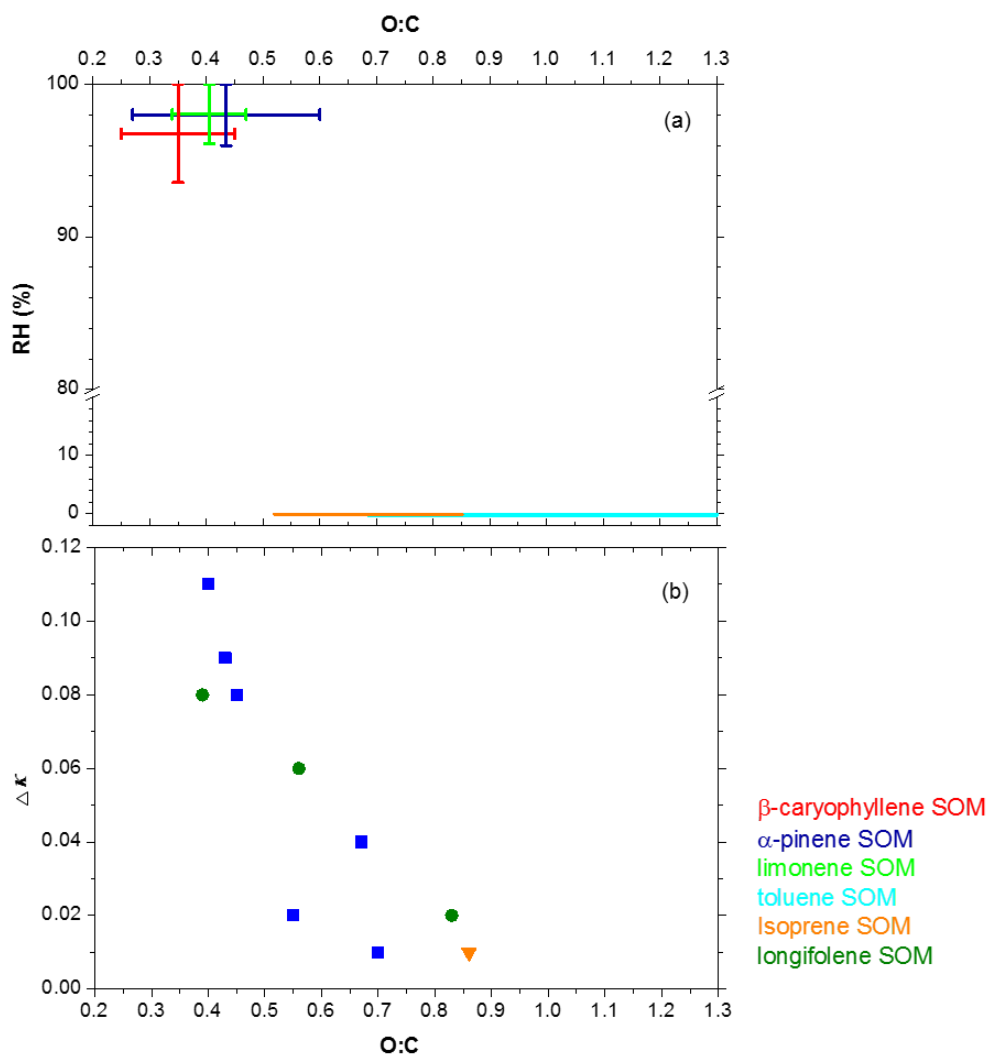
1

2

3 Figure 3. Optical images of toluene-derived SOM for the particle mass concentrations of 80 - 100
4 $\mu\text{g m}^{-3}$ (Toluene 2, Table 2) with increasing RH. Illustrations of the images are shown for clarity.
5 Green: SOM-rich phase. Size bar is 20 μm .

6

7



1

2

3 Figure 4. (a) Relative humidity in two phases as a function of the average O:C of the organic
4 material. Shown are the combined results for both increasing and decreasing relative humidity at
5 the different SOM mass concentrations from Table 3. β -caryophyllene-derived SOM (red),
6 limonene-derived SOM (light green), and toluene-derived SOM (cyan) from this study, isoprene-
7 derived SOM (orange) from Rastak et al. (2017) and α -pinene-derived SOM (blue) from Renbaum-
8 Wolff et al. (2016) as a function of O:C. RH value of 0 % indicates that LLPS did not occur. The



- 1 O:C values of the SOM particles were taken from Table 3. (b) The difference between κ_{HGF} and
- 2 κ_{CCN} , denoted as $\Delta\kappa$, as a function of the average O:C of the SOM. Data taken from Table 4.
- 3